Comparison of FBAR and QCM-D sensitivity dependence on adlayer thickness and viscosity

Nirschl, M ; Schreiter, M ; Vörös, J

Abstract: Unlike the quartz crystal microbalance, which has been used extensively for the analysis of biochemical interactions, only few measurements with biochemical adsorbent have been done with film bulk acoustic resonators (FBAR). In this paper, the FBAR behaviour on exposure to a lipid vesicle solution and the formation of a polyelectrolyte multilayer structure is investigated and compared with the results obtained with the quartz crystal microbalance. Differences in the resonator response were found between the two techniques and depending on the resonators resonance frequency ranging from the MHz to the GHz regime. As an explanation, we suggest that the penetration depth and the influence on viscoelastic properties, which are both known to be frequency dependent, cause the variations in the results. As a consequence, the higher operating resonance frequencies of the FBAR increase the sensitivity to changes in the viscoelasticity of the adsorbent and also decrease the sensing length of the device.

DOI: https://doi.org/10.1016/j.sna.2010.11.003

Comparison of FBAR and QCM-D sensitivity dependence on adlayer thickness and viscosity

Martin Nirschl[a,b,*]

Matthias Schreiter[a]

Janos Vörös[b]

[a]*Siemens AG Munich, Corporate Technology, Otto-Hahn-Ring 6, 81739 Munich, Germany*
[b]*Laboratory of Biosensors and Bioelectronics, Institute for Biomedical Engineering, ETH Zurich, Switzerland*

Abstract

Unlike the quartz crystal microbalance, which has been used extensively for the analysis of biochemical interactions, only few measurements with biochemical adsorbent have been done with film bulk acoustic resonators (FBAR). In this paper, the FBAR behaviour on exposure to a lipid vesicle solution and the formation of a polyelectrolyte multilayer structure is investigated and compared with the results obtained with the quartz crystal microbalance. Differences in the resonator response were found between the two techniques and depending on the resonators resonance frequency ranging from the MHz to the GHz regime. As an explanation, we suggest that the penetration depth and the influence on viscoelastic properties, which are both known to be frequency dependent, cause the variations in the results. As a consequence, the operating resonance frequency was found to be an important parameter for the design of acoustic resonators as sensors.

Key words: film bulk acoustic resonator, quartz crystal microbalance, lipid bilayer, lipid vesicles, polyelectrolyte multilayer

*Corresponding author: Phone: +49 89 636 55 250, Fax: +49 89 636 48131
Email addresses: martin.nirschl.ext@siemens.com (Martin Nirschl[a,b,]), matthias.schreiter@siemens.com (Matthias Schreiter[a]), janos.voros@biomed.ee.ethz.ch (Janos Vörös[b])

Comparison of FBAR and QCM-D sensitivity dependence on adlayer thickness and viscosity

Martin Nirschl[a,b,*]

Matthias Schreiter[a]

Janos Vörös[b]

[c]*Siemens AG Munich, Corporate Technology, Otto-Hahn-Ring 6, 81739 Munich, Germany*
[d]*Laboratory of Biosensors and Bioelectronics, Institute for Biomedical Engineering, ETH Zurich, Switzerland*

1. Introduction

Thickness shear mode (TSM) resonators in form of quartz crystal microbalances (QCM) have been used for decades for the analysis of intermolecular interactions (Kurosawa et al., 2006). However, TSM resonators produced by thin-film technology, namely film bulk acoustic resonators (FBAR) have been produced just recently for the application in liquid (Link et al., 2006b; Bjurström et al., 2006; Dickherber et al., 2006). Thin film bulk acoustic resonators vibrating in longitudinal mode have been produced before e.g. for filter applications (Lakin, 2005). For application in liquid, however, acoustic resonators operating in shear mode were developed as the acoustic losses caused by longitudinal waves propagating into the liquid are too high to achieve sufficient Q-factors.

Piezoelectric thin-films with the c-axis being inclined from the film normal were developed to achieve sufficiently high piezoelectric shear coupling coefficients (Wang and Lakin, 1982; Carlotti et al., 1990; Akiyama et al., 2004; Martin et al., 2005; Wingqvist et al., 2005; Link et al., 2006b; Yanagitani et al., 2007; Fardeheb-Mammeri et al., 2008)

While the working principle of FBAR and QCM is similar, the QCM is produced in a top-down process and FBARs in a bottom-up process using thin-film technology. As a result FBARs can be made thinner, which results in a higher resonance frequency. FBARs operating from some hundreds of MHz to several GHz have been presented (Lakin, 1999). The small size makes it possible to integrate many resonators on a small area, which makes the FBAR

*Corresponding author: Phone: +49 89 636 55 250, Fax: +49 89 636 48131
Email addresses: martin.nirschl.ext@siemens.com (Martin Nirschl[a,b,]), matthias.schreiter@siemens.com (Matthias Schreiter[a]), janos.voros@biomed.ee.ethz.ch (Janos Vörös[b])

a promising low-cost alternative for biomolecular interaction analysis with high throughput.

Much theoretical work is available for acoustic resonators. Starting from the linear dependence of a deposited mass in air (Sauerbrey, 1959), models were found for use of the QCM in bulk liquid (Kanazawa and Gordon, 1985) and for viscoelastic layers in air and liquid (Voinova et al., 1999; Johannsmann, 2007; Lucklum, 2005; Voinova et al., 2002; Rodahl and Kasemo, 1996). From these investigations it is known that the QCM responds to changes is the density, thickness, viscosity and elasticity of the adsorbent. Analogously, Francis et al. (2006) investigated the influence of density, thickness and viscosity of adsorbents on surface acoustic wave (SAW) sensors. They used the temperature-induced conformational changes of a polymer to model the SAW device behaviour. Wingqvist et al. (2009) specifically studied the frequency response of FBARs for protein films with thicknesses in the range of the film resonance. In these models the resonance frequency plays an important role e.g. for the influence of the adsorbed mass and the viscoelastic peoperties of the adsorbant. In order to investigate the sensor response on adlayers with different viscoelastic properties we used lipid vesicles as a model system. The resonance frequency response and dissipation change on exposure to a lipid vesicle solution has been studied intensively on QCM-D (Keller and Kasemo, 1998) and compared with other techniques such as SPR (Keller et al., 2000) and OWLS (Horvath et al., 2003). During the transition from whole vesicles to a lipid bilayer the viscoelastic properties change significantly due to the release of the solvent trapped inside the vesicles, which makes it interesting to compare this model system for acoustic resonators with different resonance frequencies.

Furthermore, the maximum thickness of the adlayer which can be detected (i.e. the sensing depth) by the sensor is frequency dependent because of the short distance acoustic waves propagate into the sensor surrounding (i.e. the penetration depth). In order to compare the sensing length of the QCM and the FBAR, we performed the layer-by-layer deposition (LBL) of a polyelectrolyte multilayer (PEM) on QCM-D and FBAR. The adsorption of PEM films has been monitored previously with QCM (Lvov et al., 1995), OWLS (Picart et al., 2002) and SPR (Caruso et al., 1998). Using an exponentially growing film thicknesses of several hundreds of nanometer, which is around the expected penetration depth, were achieved (Grieshaber et al., 2008; Wingqvist et al., 2009).

In this paper we compare QCM-D and FBAR during vesicle adsorption and bilayer formation and polyelectrolyte multilayer formation. Using these two techniques, acoustic resonators with a frequency range from 5 MHz up to about 2 GHz were available. The experimental results were underlined by simulations based on the Mason model (Mason, 1950).

1.1. Materials and methods

All adsorption measurements were performed at 25° C. All injections were done with a minimum amount of 1 ml on FBAR and 400 µl on QCM-D to ensure complete exchange of the liquids. Ultrapure water (Milli-Q gradient A

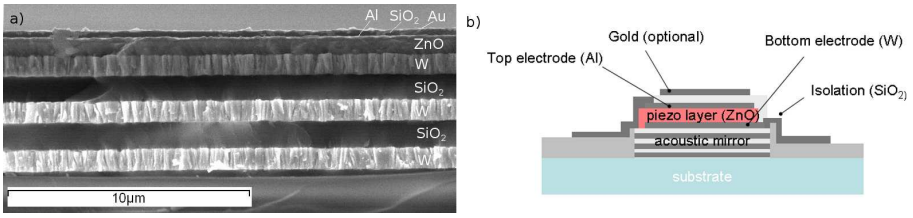

Figure 1: (a) SEM picture and (b) an illustration showing the FBAR stack: The piezoelectric ZnO is sandwiched between a aluminum top electrode and a tungsten bottom electrode. The resonator is built on top of an acoustic mirrow consisting of alternating layers of tungsten and SiO_2. The resonators is isolated from the liquid envisonment with another layer of SiO_2. Some resonators were abvailable with an additional gold layer.

10 system, Millipore Corporation, USA) was used for the preparation of all solutions.

1.1.1. FBAR

The film bulk acoustic resonators used in this study consist of a 500 nm thick piezoelectric zinc oxide layer sandwiched between a 100 nm aluminium top electrode and an 890 nm tungsten bottom electrode. The ZnO was deposited by reactive sputtering using a blind system which is described in detail in Link et al., 2006a. This deposition process formed a ZnO layer with the c-axis being inclined against the layer normal resulting in effective shear coupling coefficients of up to 19.2 %. The resonators were covered with a 300 nm thick SiO_2 layer to isolate the electrodes from the liquid and are mounted on a quarter-wavelength acoustic mirror (made of SiO_2 and W) in order to avoid acoustic waves propagating into the substrate. This configuration using an acoustic mirror is called surface mounted resonator (SMR). The resonators could be either used with the SiO_2 layer in contact with the liquid or a thin gold layer could be deposited on the SiO_2 layer to have contact with the liquid. (Figure 1)

A network analyser (Agilent 8720ES) was used to scan the electrical impedance of the resonators. The serial resonance frequency was read-out by determining the frequency with the maximum electrical conductance. The Q-factor and the resulting dissipation $D = 1/Q$ was determined following the formula $Q_s = \frac{f_s}{2} \frac{<Z}{df} \|_{f_s}$, where f_s is the serial resonance frequency and $\frac{<Z}{df} \|_{f_s}$ the inclination of the electrical impedance at resonance (Link, 2006; Link et al., 2006b). The resonator characteristics such as electrical impedance, resonance frequency and mass sensitivity could be simulated using a one-dimensional transmission line model by Mason (Mason, 1950; Rosenbaum, 1988). Resulting from the set-up described above, the fundamental resonance frequency was about 900 MHz with a simulated mass sensitivity of $1.47\,kHz\,cm^2\,ng^{-1}$ for the resonators with the SiO_2 surface and about 800 MHz with a simulated mass sensitivity of $1.32\,kHz\,cm^2\,ng^{-1}$ for the resonators with the additional gold layer. Both types of resonators had a Q-factor of around 160 in water which was sufficient for measurements in liquid environment.

From the resonators covered with gold, either the fundamental frequency or the third overtone at 2 GHz could be read-out. The Q-factor of the third overtone was at around 30 and the simulated mass sensitivity was $2.15\,kHz\,cm^2\,ng^{-1}$. Due to the significantly lower Q-factor the noise of the resonance frequency and especially the dissipation was much higher than with the fundamental.

The FBARs were cleaned in oxygen plasma for 5 minutes at 100 W before the measurements. A flow cell (about 60 µl volume) was mounted on top of the resonators. The set-up is described in detail in Weber et al., 2006.

Measurements on FBAR were performed at least in triplicates if not stated otherwise.

1.1.2. QCM-D

QCM-D (Q-Sense AB, Sweden) equipped with axial flow chamber was used. This technique is described in detail in (Marx, 2003). The change of the resonance frequency Δf and dissipation change ΔD were monitored for several harmonics (5, 15, 25, 35, 45, 55 and 65 MHz) simultaneously. In all diagrams, the normalised frequency shift ($\Delta f_n = \frac{\Delta f}{n}$, where n is the overtone number) is shown.

Prior to their use, the crystals were cleaned for 30 minutes in 2% Sodium Dodecyl Sulphate (SDS) solution and 30 minutes in an UV/Ozone cleaner.

1.1.3. Simulation

Qtools software (Q-Sense AB, Sweden) was used to receive material properties (e.g. thickness and viscosity) of the adsorbents measured by QCM. The Mason model was used to simulate the frequency response of both QCM-D and FBAR to adsorbents with different thickness, density, viscosity and elasticity in liquid. The model is described in detail in Link (2006).

1.1.4. Vesicle preparation

1,2-di-oleoyl-sn-glycero-3-phosphocholine (DOPC) phospholipids were purchased from Avanti Polar Lipids Inc., USA and stored dissolved in chloroform at -20°C. The chloroform was evaporated using dry nitrogen; buffer was added and extruded 31 times through polycarbonate membranes with a pore size of 50 nm. The buffer used was 20 mM 4-(2-hydroxyethyl)piperazine-1-ethane-sulfonic acid (HEPES, Fluka Chemie GmbH, Switzerland), 150 mM $NaCl$ and 2 mM of $CaCl_2$. The concentration of the vesicles was 0.1 mg/ml.

1.1.5. Polyelectrolyte multilayer

The polyelectrolyte multilayer built on QCM-D and FBAR was $PEI - (PGA - PAH)_n$. The sensors where exposed to poly-ethylenimine (PEI), Poly-L-Glutamic acid (PGA) and Poly-(allylamine hydrochloride) (PAH). The polyelectrolytes were injected in time intervals of 5 minutes at a concentration of 1 mg/ml without flow and without buffer rinse between the injections as shown in Grieshaber et al., 2008. The buffer used was 10 mM HEPES solution containing 100mM KCl, pH adjusted to 7.4.

1.2. Results

1.2.1. Vesicle adsorption and bilayer formation

Measurements on QCM-D were performed on both gold and SiO_2 surfaces as a reference for the FBAR measurements. On SiO_2, during vesicle adsorption, the resonance frequency decreased until a critical surface concentration was reached about 100 seconds after injection. At this point, the vesicles formed a lipid bilayer, which brought the dissipation closely back to zero, and the frequency increased up to a frequency of about -25 Hz (Figure 2a) which is characteristic for a lipid bilayer. On gold, after exposure to the vesicle solution, a monotonous decrease of the resonance frequency was observed. The saturation values for both the frequency shift and the dissipation change are several times higher on the gold surface than on the SiO_2 surface (Figure 2b). The adsorption on both gold and SiO_2 was as expected from literature (Keller and Kasemo, 1998).

The measurements were conducted in the same way using the FBAR with SiO_2 and gold surfaces. On gold, vesicle adsorption analogously to the QCM-D measurements could be observed. The resonance frequency decreased and dissipation increased with addition of the vesicles (Figure 2d).

On SiO_2, vesicle adsorption caused the dissipation to increase for a short time and in the following decreasing back close to the original value (Figure 2c). While this indicates a vesicle adsorption and subsequent bilayer transformation, the non-monotonic behaviour of the frequency response of the QCM-D curve cannot be seen in the FBAR measurement (Figure 2a and 2c). The frequency shift at saturation was 483 kHz $\pm$ 151 kHz on gold and 592 kHz $\pm$ 139 kHz on SiO_2 surface.

For the resonators with the gold surface, the vesicle adsorption was also performed with the third overtone at 2 GHz. However, due to the low Q-factor of this overtone the noise of the dissipation was higher than the signal expected from vesicle adsorption, therefore the adsorption could only be observed from the change in resonance frequency. The frequency shift at saturation was 305 kHz $\pm$ 105 kHz and thus lower than the shift of the fundamental frequency while from the simulation the overtone is expected to have a higher mass sensitivity (Figure 2e, Figure 4a).

The frequency shifts at saturation for all measurements were converted into surface mass using the Sauerbrey equation for the measured values from QCM-D (Sauerbrey, 1959) and the Mason model for the values from the FBAR (Figure 2f). It can be seen that the calculated mass decreases with higher frequencies in case of the vesicles while it nearly stays constant for the lipid bilayer. Interestingly, while the Sauerbrey mass is higher for the vesicles than the lipid bilayer on QCM-D as expected it is the other way round on the FBAR.

1.2.2. Polyelectrolyte multilayer

The deposition of the polyelectrolyte multilayer on QCM-D was followed by a monotonic decrease of the resonance frequency with increasing layer number. On the other hand, the dissipation increased after PGA and decreased after PAH

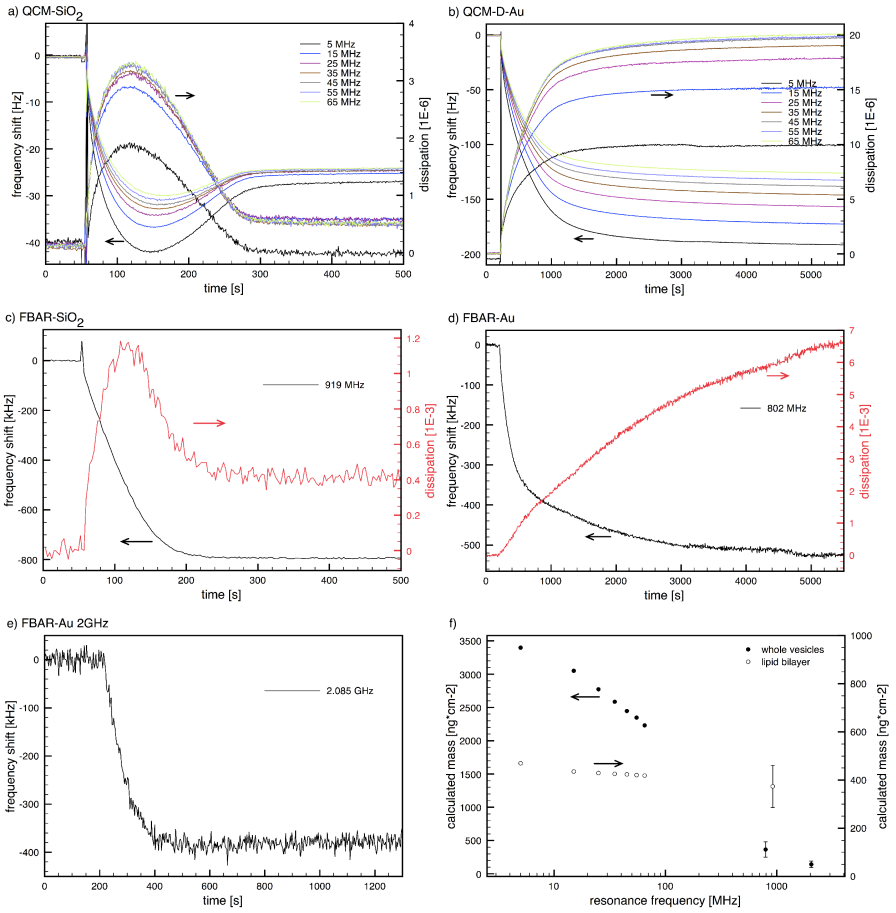

Figure 2: Comparison of vesicle adsorption and bilayer formation as measured by FBAR and QCM-D: Lipid bilayer formation on SiO_2 monitored by the frequency shift and dissipation change using QCM-D (a) and FBAR (c). Adsorption of intact vesicles on gold measured by QCM-D (b) and FBAR at a resonance frequency of 800 MHz (d) and 2 GHz (e). Surface mass calculated from the frequency shift and plotted for lipid bilayer and the vesicle layer for all frequencies from 5 MHz to 2 GHz. The error bars show the standard deviation over three measurements. (f)

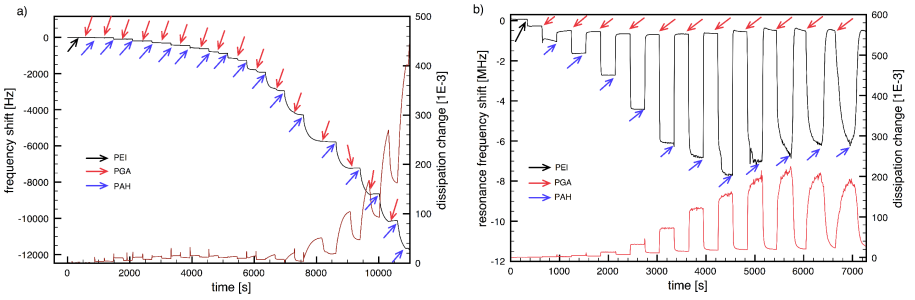

Figure 3: Polyelectrolyte multilayer formation on QCM-D (a) and FBAR (b) Black arrows indicate the injection of PEI, red arrows injection of PGA and blue of PAH. While the frequency decreases monotonously on QCM-D, on FBAR large jumps appear at every injection.

addition in accordance with the literature (Wagberg et al., 2004; Boulmedais et al., 2003; Grieshaber et al., 2008). This indicates a more rigid film in case of PAH being added the last (Figure 3a).

The PEM film was built in the same manner on the FBAR like on the QCM-D. It could be observed that the frequency decreases after addition of PGA until the 7^{th} layer pair. From the 8^{th} layer pair on the frequency increases again in respect to the previous PGA injection. On the contrary, after the addition of PAH, the frequency increases rapidly to a much smaller frequency shift. The dissipation was high after adding PGA and lower after adding PAH (Figure 3b), which is the opposite to the QCM-D measurement.

1.3. Discussion

The measurements showed that vesicle adsorption and lipid bilayer formation and the LBL deposition of PEMs could be observed on FBAR and that significant differences were found for different resonance frequencies.

We suggest, that the increased resonance frequency of the FBAR causes the deviation from the QCM-D which operates at lower frequencies. At a higher resonance frequency, the penetration depth δ is lower according to $\delta = \sqrt{\frac{\eta}{\pi \rho f_0}}$, where η is the viscosity and ρ the density of the surrounding medium. δ determines the distance where the resonator is sensitive. Normally, for thin adlayers, the penetration depth is mostly determined by the solvent. However, for thick films and high frequencies the adlayer might be thicker than δ (Wingqvist et al., 2009).

The viscosity and density of the layers can be estimated from the QCM-D measurements ($\eta_{vesicles} = 1.14 * 10^{-3} \frac{kg}{ms}$ and $\rho_{vesicles} = 1030 \frac{kg}{m^3}$). Assuming that the viscosity is frequency independent the resulting penetration depth would be 265 nm at 5 MHz, 69 nm at 75 MHz and at the FBAR operating frequency of 800 MHz it is around 21 nm. For the overtone at 2 GHz it would be only 13 nm. In the QCM-D measurements the penetration depth is higher than the thickness of both the lipid bilayer and the whole vesicles. Therefore the

sensor response is related to the whole vesicle including the coupled water. As such, the calculated mass is much higher than in case of the lipid bilayer. (Keller et al., 2000) On the FBAR, however, the penetration depth is smaller than the 50 nm diameter of the vesicles. As a result, the vesicles are only partially penetrated by the acoustic waves and as such only part of the vesicles contribute to the frequency shift. The height of the frequency shift is determined by the fraction of the vesicle and coupled water penetrated by the acoustic wave and by the packing density of the adsorbed vesicles. The lipid bilayer instead is completely within the sensing depth, therefore all of its mass contributes to the frequency shift. This explains why we obtained a larger mass for the bilayer than for the vesicles at 800 MHz (Figure 2f). The dissipation change still shows the vesicle rupture event, probably because of the change in viscoelastic properties of the part of the vesicles penetrated by the acoustic waves (Figure 2c,2d and 4c).

The influence of the penetration depth helps also to explain the frequency shift obtained at 2 GHz. The simulated mass sensitivity is higher for the mode at 2 GHz than for the one at 800 MHz, but the frequency shift of the adsorbed vesicles was smaller for the overtone at 2 GHz. This is because the penetration depth is 13 nm at 2 GHz which leaves even a larger part of the vesicles "unseen" by the resonator, and only a small part contributes to the resonance frequency shift.

In order to better understand the consequences of the altered penetration depth at different frequencies we have simulated the expected frequency shifts upon adsorption of homogeneous layers with different thicknesses. Figure 4a shows the simulated frequency shifts of a viscoelastic layer with viscosity and density of $\eta_{vesicles}$ and $\rho_{vesicles}$. The simulation indicates remarkable differences between QCM-D and FBAR, e.g. the critical thickness at which the frequency shift has a maximum is very different.

Another situation when the sensor response depends on the resonance frequency is related to the influence of the viscoelastic properties of the adsorbent. The frequency is not only influenced by the mass attachment itself but also by the viscosity and elasticity of the adsorbed layer. The frequency shift and dissipation caused by a viscoelastic layer deposited on an acoustic resonator operated in bulk liquid has been described as the result of three contributions: The bulk liquid (Kanazawa and Gordon, 1985), the mass of the adsorbent (Sauerbrey, 1959) and the viscoelastic properties of the adsorbent (Voinova et al., 2002). The viscoelastic properties contain the viscosity, which cannot be assumed to be constant over the broad frequency range from MHz to GHz. A generalised model for the complex shear modulus has been introduced in the form $G^* = \frac{G}{(1-\frac{i}{\omega\tau})^b}$ by Voinova et al., 2002. The complex shear modulus was considered as the result of a distribution of relaxation times τ characterised by the factor b and the resonance frequency ω. Following this model, we suggest that for the adsorbed vesicles the distribution of relaxation times allows excitation at low frequencies while the relaxation times are too high to allow sufficient excitation at the higher resonance frequency of the FBAR. In this way, the contribution of the viscoelastic properties to the frequency shift is small compared

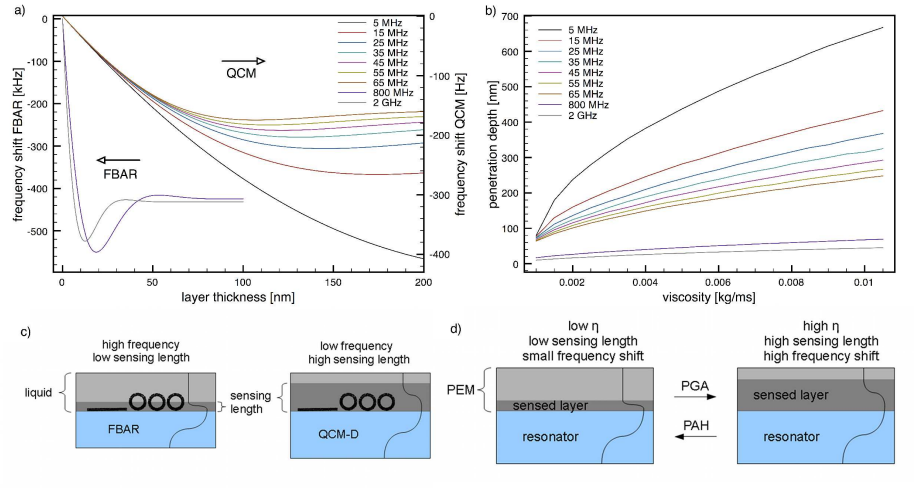

Figure 4: a) Calculated adsorption of a viscoelastic layer on QCM and FBAR for different frequencies. The penetration depth is significantly different between the two techniques and for different resonance frequencies. The sketch in c) illustrates the impact of the different penetration depths on the vesicle adsorption: The whole vesicles are penetrated by the acoustic waves on QCM-D while the sensing depth is shorter than the vesicle diameter on FBAR. b) The sensing depth (i.e. layer thickness at maximum frequency shift) for different viscosities of a 150 nm thick adlayer. With lower viscosity and higher frequencies the sensing depth decreases. d) The sketch illustrates the mechanism causing the high frequency jumps on FBAR, the change in the viscosity of the PEM moves mass in an out of the sensing depth.

to the contribution of the mass attachment. The real and the imaginary part of G^* have a different frequency dependency depending on the distribution of relaxation times, so that the influence on the dissipation can be high while it is low on the resonance frequency. Thus, the transition from whole vesicles to lipid bilayer cannot be seen from the frequency shift but only from the difference in dissipation between the whole vesicle, which is the at least partially "seen" by the resonator, and the lipid bilayer. The fact that frequency shift and dissipation do not necessarily behave in an analogue manner can also be seen from the vesicle adsorption on QCM-D, where the frequency shift at saturation decreases while the dissipation increases at higher frequencies (Figure 2b).

Further differences between QCM-D and FBAR could be seen from the polyelectrolyte multilayer deposition. On QCM-D, increasing film thickness caused a decrease in frequency shift. On FBAR, the frequency decreased only by adding PGA. After adding PAH the frequency went quickly back. The dissipation change shows alternately a high and a low dissipative layer in opposite to the QCM-D measurement (Figure 3). From previous work (Notley et al., 2005) it is known that the PEM's viscosity depends on which polymer was added last. This change in viscosity on the other hand has a large influence on the penetration depth. In Figure 4b) the sensing depth is plotted for different viscosities for a 150 nm thick adlayer, where the thickness at which the maximum frequency

shift was chosen to be the sensing depth. It can be seen that the sensing depth of the FBAR is smaller than the thickness of the adlayer. This means that if changes in the viscosity alter the sensing depth the proportion of the PEM which is sensed by the resonator will also be different. The part of the adsorbant moved out of the sensing depth does not contribute to the resonance frequency and dissipation change. By changing the viscosity and thus the sensing length within the PEM, the mass between the two sensing lengths is moved in and out of the sensing length of the resonator causing the big changes in frequency and dissipation. The sketches in Figure 4d) illustrate this process.

From Figure 3b) it can be seen that the maximum frequency shift, which we assume to be the penetration depth, is reached after the 5th layer for the PGA and for the 7 th layer for the PAH. From the QCM-D measurements the corresponding thickness was calculated to be 80 nm for the PGA and 210 nm for the PAH. Assuming that the PEM is a homogeneous stack with a density of $1100\frac{kg}{m^3}$ for both polymers we receive an estimated viscosity for the PEM of $\eta_{PGA} = 17.7 * 10^{-3}\frac{kg}{ms}$ if PGA is the last layer and $\eta_{PAH} = 122 * 10^{-3}\frac{kg}{ms}$ if PAH is the last layer.

1.4. Conclusion

In this paper, we have compared the sensor response of the FBAR with QCM-D on the adsorption of vesicles and the formation of a lipid bilayer and the LBL deposition of PEMs. We have shown that there are significant differences between the two different types of acoustic resonators and between different resonance frequencies. We have suggested that in the measurements we have done, the decreased penetration depth and the smaller influence of viscoelastic properties at higher frequency caused the unexpected results. This hypothesis was confirmed by simulations using the Mason model.

As a result, in this paper we have shown, that the properties of the adsorbent (e.g. thickness, viscoelastic properties) have to be taken into consideration when selecting the resonance frequency of acoustic resonators as mass sensors in order to be able to efficiently sense the adsorbent. While a higher resonance frequency makes the device thinner and more sensitive, the frequency has an upper limit where the sensing length of the device becomes too short, e.g. because the assay to be used has a thickness in the range of the sensing length. However, in an application where a high sensitivity to changes in the viscosity is desired the operating frequency might be selected in a range where the adsorbent has a thickness near the sensing length, as it was the case for the measurements in this paper.

Acknowledgement

We thank Raphael Zahn for the help with the polyelectrolytes, Dorothee Grieshaber and Marta Bally for the help with the QCM-D and the vesicle preparation and Fredrik Höök for helpful discussion.

References

Akiyama, M., Nagao, K., Ueno, N., Tateyama, H., Yamada, T., 2004. Influence of metal electrodes on crystal orientation of aluminum nitride thin films. Vacuum 74 (3-4), 699 – 703, selected papers revised from the Proceedings of the Seventh International Symposium on Sputtering and Plasma Processes (ISSP 2003).

Bjurström, J., Wingqvist, G., Katardjiev, I., Nov 2006. Synthesis of textured thin piezoelectric aln films with a nonzero c-axis mean tilt for the fabrication of shear mode resonators. IEEE Trans Ultrason Ferroelectr Freq Control 53 (11), 2095–2100.

Boulmedais, F., Ball, V., Schwinte, P., Frisch, B., Schaaf, P., Voegel, J.-C., Jan. 2003. Buildup of exponentially growing multilayer polypeptide films with internal secondary structure. Langmuir 19 (2), 440–445.

Carlotti, G., Fioretto, D., Socino, G., Palmieri, L., Petri, A., Verona, E., 4–7 Dec. 1990. Surface acoustic waves in c-axis inclined zno films. In: Proc. Ultrasonics Symposium IEEE 1990. pp. 449–453.

Caruso, F., Furlong, D. N., Ariga, K., Ichinose, I., Kunitake, T., Aug. 1998. Characterization of polyelectrolyte-protein multilayer films by atomic force microscopy, scanning electron microscopy, and fourier transform infrared reflection?àíabsorption spectroscopy. Langmuir 14 (16), 4559–4565.

Dickherber, A., Corso, C. D., Hunt, W., 2006. Lateral field excitation (lfe) of thickness shear mode (tsm) acoustic waves in thin film bulk acoustic resonators (fbar) as a potential biosensor. Conf Proc IEEE Eng Med Biol Soc 1, 4590–4593.

Fardeheb-Mammeri, A., Assouar, M., Elmazria, O., Gatel, C., Fundenberger, J.-J., Benyoucef, B., 2008. c-axis inclined aln film growth in planar system for shear wave devices. Diamond and Related Materials 17 (7-10), 1770 – 1774, proceedings of Diamond 2007, the 18th European Conference on Diamond, Diamond-Like Materials, Carbon Nanotubes, Nitrides and Silicon Carbide - Diamond 2006, Proceedings of Diamond 2007, the 18th European Conference on Diamond, Diamond-Like Materials, Carbon Nanotubes, Nitrides and Silicon Carbide.

Francis, L.A., Friedt, J., Zhou, C., Bertrand, P., 2006. In Situ Evaluation of Density, Viscosity, and Thickness of Adsorbed Soft Layers by Combined Surface Acoustic Wave and Surface Plasmon Resonance. Analytical Chemistry 78 (12), 4200–4209.

Grieshaber, D., Vörös, J., Zambelli, T., Ball, V., Schaaf, P., Voegel, J.-C., Boulmedais, F., Dec 2008. Swelling and contraction of ferrocyanide-containing polyelectrolyte multilayers upon application of an electric potential. Langmuir 24 (23), 13668–13676.

Horvath, R., Fricsovszky, G., Papp, E., 2003. Application of the optical waveguide lightmode spectroscopy to monitor lipid bilayer phase transition. Biosensors and Bioelectronics 18 (4), 415 – 428.

Johannsmann, D., 2007. Studies of viscoelasticity with the qcm. Piezoelectric Sensors, 49–109.

Kanazawa, K. K., Gordon, J. G., 1985. Frequency of a quartz microbalance in contact with liquid. Analytical Chemistry 57 (8), 1770–1771.

Keller, C., Kasemo, B., Sep. 1998. Surface specific kinetics of lipid vesicle adsorption measured with a quartz crystal microbalance.

Keller, C. A., Glasmästar, K., Zhdanov, V. P., Kasemo, B., Jun 2000. Formation of supported membranes from vesicles. Phys Rev Lett 84 (23), 5443–5446.

Kurosawa, S., Park, J.-W., Aizawa, H., Wakida, S.-I., Tao, H., Ishihara, K., Oct 2006. Quartz crystal microbalance immunosensors for environmental monitoring. Biosens Bioelectron 22 (4), 473–481.

Lakin, K., 1999. Thin film resonators and filters. Ultrasonics Symposium, 1999. Proceedings. 1999 IEEE 2, 895–906 vol.2.

Lakin, K. M., May 2005. Thin film resonator technology. IEEE Trans Ultrason Ferroelectr Freq Control 52 (5), 707–716.

Link, M., 2006. Study and realization of shear wave mode solidly mounted film bulk acoustic resonators (fbar) made of caxis inclined zinc oxide (zno) thin films: application as gravimetric sensors in liquid environments. Ph.D. thesis, Université Henri Poincaré, Nancy I.

Link, M., Schreiter, M., Weber, J., Gabl, R., Pitzer, D., Primig, R., Wersing, W., Assouar, M. B., Elmazria, O., 2006a. c-axis inclined zno films for shear-wave transducers deposited by reactive sputtering using an additional blind. Journal of Vacuum Science & Technology A: Vacuum, Surfaces, and Films 24 (2), 218–222.

Link, M., Schreiter, M., Weber, J., Primig, R., Pitzer, D., Gabl, R., Feb 2006b. Solidly mounted zno shear mode film bulk acoustic resonators for sensing applications in liquids. IEEE Trans Ultrason Ferroelectr Freq Control 53 (2), 492–496.

Lucklum, R., Nov 2005. Non-gravimetric contributions to qcr sensor response. Analyst 130 (11), 1465–1473.

Lvov, Y., Ariga, K., Ichinose, I., Kunitake, T., Jun. 1995. Assembly of multicomponent protein films by means of electrostatic layer-by-layer adsorption. Journal of the American Chemical Society 117 (22), 6117–6123.

Martin, F., Jan, M. E., Rey-Mermet, S., Su, D., Muralt, P., Cantoni, M., 18–21 Sept. 2005. Shear mode coupling and tilted grain growth of a1n thin films in baw resonators. In: Proc. IEEE Ultrasonics Symposium. Vol. 1. pp. 333–336.

Marx, K. A., 2003. Quartz crystal microbalance: a useful tool for studying thin polymer films and complex biomolecular systems at the solution-surface interface. Biomacromolecules 4 (5), 1099–1120.

Mason, W., 1950 1950. Piezoelectric crystals and their application to ultrasonics. D.Van Nostrand Co., McMillan and Co., London, New York, UK.

Notley, S. M., Eriksson, M., Wagberg, L., 2005. Visco-elastic and adhesive properties of adsorbed polyelectrolyte multilayers determined in situ with qcm-d and afm measurements. Journal of Colloid and Interface Science 292 (1), 29 – 37.

Picart, C., Mutterer, J., Richert, L., Luo, Y., Prestwich, G. D., Schaaf, P., Voegel, J.-C., Lavalle, P., 2002. Molecular basis for the explanation of the exponential growth of polyelectrolyte multilayers. Proceedings of the National Academy of Sciences of the United States of America 99 (20), 12531–12535.

Rodahl, M., Kasemo, B., 1996. On the measurement of thin liquid overlayers with the quartz-crystal microbalance. Sensors and Actuators A: Physical 54 (1-3), 448 – 456.

Rosenbaum, J. F., 1988. Bulk Acoustic Wave Theory and Devices. Artech House, Inc.

Sauerbrey, G., Apr. 1959. Verwendung von schwingquarzen zur wägung dünner schichten und zur mikrowägung. Zeitschrift für Physik A Hadrons and Nuclei 155 (2), 206–222.

Voinova, M. V., Jonson, M., Kasemo, B., Oct 2002. Missing mass effect in biosensor's qcm applications. Biosens Bioelectron 17 (10), 835–841.

Voinova, M. V., Rodahl, M., Jonson, M., Kasemo, B., 1999. Viscoelastic acoustic response of layered polymer films at fluid-solid interfaces: Continuum mechanics approach. Physica Scripta 59 (5), 391–396.

Wagberg, L., Pettersson, G., Notley, S., 2004. Adsorption of bilayers and multilayers of cationic and anionic co-polymers of acrylamide on silicon oxide. Journal of Colloid and Interface Science 274 (2), 480 – 488.

Wang, J. S., Lakin, K. M., 1982. Sputtered c-axis inclined zno films for shear wave resonators. In: Proc. Ultrasonics Symposium. pp. 480–483.

Weber, J., Albers, W. M., Tuppurainen, J., Link, M., Gabl, R., Wersing, W., Schreiter, M., 2006. Shear mode fbars as highly sensitive liquid biosensors. Sensors and Actuators A: Physical 128 (1), 84 – 88.

Wingqvist, G., Anderson, H., Lennartsson, C., Weissbach, T., Yantchev, V., Spetz, A. L., 2009. On the applicability of high frequency acoustic shear mode biosensing in view of thickness limitations set by the film resonance. Biosensors and Bioelectronics 24 (11), 3387 – 3390.

Wingqvist, G., Bjurstrom, J., Liljeholm, L., Katardjiev, I., Spetz, A. L., Oct. 30 2005–Nov. 3 2005. Shear mode aln thin film electroacoustic resonator for biosensor applications. In: Proc. IEEE Sensors. p. 4pp.

Yanagitani, T., Kiuchi, M., Matsukawa, M., Watanabe, Y., Aug 2007. Characteristics of pure-shear mode baw resonators consisting of (1120) textured zno films. IEEE Trans Ultrason Ferroelectr Freq Control 54 (8), 1680–1686.